

REVIEW

**Comparative study of the active sites in zeolites by different probe molecules**

VERA DONDUR<sup>1\*#</sup>, VESNA RAKIĆ,<sup>2</sup> LJILJANA DAMJANOVIĆ<sup>1#</sup> and ALINE AUROUX<sup>3</sup>

<sup>1</sup>Faculty of Physical Chemistry, Studentski trg 12-16, 11000 Belgrade, Serbia and Montenegro, (e-mail: edondur@ffh.bg.ac.yu), <sup>2</sup>Faculty of Agriculture, Nemanjina 6, 11080 Belgrade-Zemun, Serbia and Montenegro and <sup>3</sup>Institut de Recherches sur la Catalyse, 2 Av. A. Einstein, 69626 Villeurbanne, France

(Received 14 Decembar 2004)

*Abstract:* This review summarizes some of the recently published results concerning the acid sites in the zeolites ZSM-5 and Y studied by temperature-programmed desorption (TPD) and adsorption calorimetry using different probe molecules NH<sub>3</sub>, CO, N<sub>2</sub>O and *n*-hexane. For the first time it has been shown that the acid sites in hydrated zeolites are accessible for *n*-hexane adsorption.

*Keywords:* zeolites, temperature-programmed desorption, microcalorimetry, acid sites, ammonia adsorption, carbon monoxide adsorption, nitric oxide adsorption, *n*-hexane adsorption.

1. INTRODUCTION

Zeolites have been the subject of tremendous interest of both the scientific and industrial world. They are used on a large industrial scale for a great variety of processes, from simple drying to complicated catalytic reactions.<sup>1</sup> In the last decade, green chemistry has been recognized as a new approach to scientifically based environmental protection, and catalysis has manifested its role as a fundamental tool in pollution prevention.<sup>2</sup> Zeolites are also well known as environmentally friendly catalysts. Due to the diversification of the application for which these catalysts are employed, considerable research has been focused on the characterization of the active sites,<sup>3</sup> a key property for applications in catalysis.

One important topic in the research of zeolites is the characterization of the Brønsted and Lewis acid centers. Brønsted acid sites (BAS) are assigned to bridging hydroxyl groups, while Lewis acid sites (LAS) are essentially electron acceptor centers and they can be cations or different aluminium species located in defect centers; the latter ones are known as so-called true Lewis sites.

\* Author for correspondence.

# Serbian Chemical Society active member.

Various techniques have been successfully applied to study the nature, concentration, strength and strength distribution of the active sites present in zeolites.<sup>4</sup> Most of these methods are based on the adsorption of gas-phase probe molecules, which are chosen on the basis of their reactivity and molecular size.<sup>5–7</sup> Conventional methods, such as temperature-programmed desorption (TPD)<sup>8–17</sup> and adsorption calorimetry<sup>18–28</sup> of adsorbed probe molecules give information regarding the strength and distribution of the active sites. Spectroscopic methods, such as infrared<sup>29–39</sup> and NMR spectroscopy,<sup>40–41</sup> have been widely used to study the nature of the acid sites found on zeolites and other solid acids. It has been shown as highly informative to combine TPD and microcalorimetry with IR spectroscopy to investigate the interaction of gaseous probe molecules with a solid surface in order to obtain complementary results about the active sites.<sup>42–45</sup>

Two main types of probe molecules have been developed.<sup>46</sup> The probe molecules such as NH<sub>3</sub>, pyridine and amines form a chemical bond with the protons of the hydroxyl groups, thus giving information about the concentration of the acid sites of zeolites. On the other hand, aromatics, olefins, CO and H<sub>2</sub>S can be used to acquire information on the strength and the accessibility of the acid sites to the probe molecules. The equilibrium data include contributions from donor–acceptor, dispersion and non-specific polar interaction of the probe molecules with the active sites of the zeolites. However, in spite of tremendous scientific contributions, the role, the nature and the strength of acid sites in solid catalysts have been the subject of a dispute which is far from being settled and the search for a judicious molecular probe is still of vital interest. The criteria for the selection of probe molecules have been summarized in an excellent review by Knozinger.<sup>46</sup>

The applications of different probe molecules have greatly enlarged the amount of available information on the acidity of zeolites. Different molecules can probe different types of acid sites. Therefore, the application of many different probe molecules for the study of the characteristics of the active sites seems to be an appropriate method to obtain information about the activity of one solid catalyst. Weakly interacting probe molecules are much more specific than strongly interacting ones and, therefore, can provide more detailed information about the acid sites. Recently, growing attention has been paid to the study of the acid-base properties of zeolites using weakly interacting probe molecules such as N<sub>2</sub>O,<sup>47–50</sup> benzene,<sup>51</sup> CO,<sup>50–57</sup> hexane,<sup>58–62</sup> N<sub>2</sub> and H<sub>2</sub>.<sup>63,64</sup>

In this paper we review the investigation of the acid sites of two different types of zeolites, ZSM-5 and Y, using ammonia, carbon monoxide, nitric oxide and *n*-hexane as probe molecules. Although both type of zeolites having different charge-balancing cations have been investigated,<sup>28</sup> here the results obtained for samples with H<sup>+</sup> and Cu<sup>2+</sup> as the charge-balancing cations are presented. The adsorption of the chosen probe molecules enabled both strong and weak acid sites. For this purpose, both the adsorption and desorption of the mentioned probes were

studied applying microcalorimetry (MC) and temperature programmed desorption with mass spectrometer as the detector (TPD/MAS). *n*-Hexane was co-adsorbed on samples on which water molecules had been pre-adsorbed. It is shown for the first time that acid sites in hydrated zeolites are accessible for *n*-hexane. Also, it was found that some active sites in the Y and ZSM-5 zeolites strongly adsorb molecular *n*-hexane even though the zeolites were covered with water. Unusually strong adsorption of *n*-hexane on hydrated zeolites seems to be an important finding for designing new catalytic processes.

## 2. EXPERIMENTAL

### 2.1. Materials

The samples used in this investigation were prepared from synthetic FAU-type zeolites, NaY(SK-40) [Na<sub>56</sub>(AlO<sub>2</sub>(AlO<sub>2</sub>)<sub>56</sub>(SiO<sub>2</sub>)<sub>136</sub>), produced by Union Carbide Corp. The dealumination procedure was performed following a procedure described elsewhere.<sup>65</sup> Na<sub>2</sub>H<sub>2</sub>EDTA was added directly to a slurry of the initial NaY zeolite in water and stirred at 90 °C. The concentration of the dealumination agent and the contact time were varied. The cation-exchanged Cu<sup>2+</sup> samples were obtained by conventional ion-exchange procedures.<sup>44</sup> The parent Na-ZSM-5 zeolites (Si/Al = 28–120) was self-synthesized and its crystallinity was confirmed by the XRD technique. The H form of ZSM-5 zeolite was obtained following a standard procedure of ion exchange with NH<sub>4</sub>Cl and calcination at 500 °C under vacuum for 4 h. The set of the hydrogen form of ZSM-5 zeolite samples is denoted as HZSM-(*x*), where *x* indicates the Si/Al ratio. The ion exchange was performed following a procedure described in detail elsewhere.<sup>66</sup> In brief, an aqueous Cu(II) acetate solution (0.01 M, pH = 5.5–5.6) was stirred with Na-ZSM-5 for 24 h at room temperature. The samples exchanged with Cu are denoted as CuZSM-(*x*), where here, *x* represents the % of ion exchange. The results of the chemical analysis of the investigated samples are presented in Table I.

TABLE I Chemical composition of the investigated samples

Sample	Si/Al	Cu/Al	Ion-exchange (%)
HY	2.4		
HDY1	2.6		
HDY2	2.7		
HZSM-(28)	2.8		
HZSM-(40)	40		
HZSM-(80)	80		
HZSM-(120)	120		
CuY	2.4	0.375	75
CuZSM-(79)	50	0.385	79
CuZSM-(128)	50	0.640	128
CuZSM-(150)	50	0.750	

### 2.2. Temperature programmed desorption (TPD)

The amount and strength distribution of the active sites were estimated by temperature programmed desorption (TPD) of ammonia, carbon monoxide and *n*-hexane.

The temperature programmed desorption of  $\text{NH}_3$  and of *n*-hexane from HZSM samples were performed using Setaram DSC 111 differential scanning calorimeter consisting of a quartz micro-reactor, heated in a vertical furnace. An online mass spectrometer (MS, Thermostar from Pfeifer), having a capillary-coupling system, was used as the detector. Typically, 0.01 g of sample with previously adsorbed gas was placed in the reactor and purged with helium at either 100 °C for 1 h (for ammonia desorption), or 25 °C for 30 min (for *n*-hexane desorption) in order to ensure complete removal of physisorbed gases. Desorption of ammonia was then carried out from 100 to 700 °C, under helium. The interaction on *n*-hexane with the investigated zeolites was investigated after saturation of the samples with water. Temperature programmed heating was applied, without previous activation of the samples. The hydrated samples were stored for 24 h in a desiccator containing liquid *n*-hexane in an open vessel and then sample was placed in the previously described DSC/MS (Setaram/Pfeifer) equipment. Desorption was carried out from 25 to 300 °C, in a helium flow.

The experimental set-up applied for the TPD of CO and  $\text{NH}_3$  in the case of HY and de-aluminated HY samples, consists of a flow measuring and switching system and a cylindrical furnace, controlled by a linear temperature programmer (Omega CN 2010) with a quartz tube inside, in which the sample is placed. The equipment and procedure have been fully described elsewhere.<sup>44</sup> Briefly, the outlet of the TPD cell is on-line connected with a mass spectrometer (Sensorlab 200D-VG Quadrupoles), *via* a heated silica capillary tube with a fast response at 1 bar sampling pressure. For the adsorption of either CO or  $\text{NH}_3$  the same masses of samples (0.15 g in the case of CO, 0.05 in the case of  $\text{NH}_3$ ) were employed. Typically, the sample was thermally treated at 400 °C for 2 h in a helium flow. Subsequently, it was cooled (to 100 °C for ammonia adsorption or to 25 °C for CO adsorption) and either a 5 %  $\text{NH}_3/\text{He}$  or 10 %  $\text{CO}/\text{He}$  mixture was used to adsorb the regimed gas onto the sample for 30 min at the corresponding temperature. The mass spectrometer signal was properly calibrated by using dilute gas streams of known concentrations. Prior to desorption, the sample was purged with helium at the temperature of adsorption for 40 min, in order to ensure complete removal of physisorbed gas. TPD was then carried out from 100 to 800 °C under helium.

In this study, the masses 28 (CO), 18, 17 and 16 ( $\text{H}_2\text{O}$ ) were recorded. In the case of *n*-hexane TPD, the common mass fragmentation of this molecule (86, 57, 56, 55, 43, 42, 41, 27, 39) were recorded, and some additional masses (59, 58, 45, 44, 29, 28, 27). For the detection of ammonia, the mass spectrometer was set at  $m/e = 15$  in order to avoid the interference of water fragmentations masses.

In all TPD/MAS experiments the heating rate was  $10 \text{ K min}^{-1}$ , while the flow rates of either the inert or reactive gas were ( $30 \text{ ml min}^{-1}$ ).

### 2.3. Microcalorimetry

A well-established stepwise procedure, previously fully described,<sup>24,26,28,66</sup> was followed. The heats of adsorption were measured in a heat-flow microcalorimeter of the Tian-Calvet type (C80 from Setaram) linked to a glass volumetric line which permits the introduction of successive small doses of adsorbed gas. Prior the adsorption, the samples were heated overnight under vacuum at 400 °C (CO or  $\text{N}_2\text{O}$ ). Successive small doses of the required gas were introduced onto the samples until a final equilibrium pressure of 66 Pa was achieved. The equilibrium pressure corresponding to each adsorbed amount was measured by means of a differential pressure gauge from Datametrics. Subsequently, the sample was pumped, the desorption peak recorded and re-adsorption performed at the temperature of adsorption. The irreversibly adsorbed amount of chemisorbed gas was calculated from difference between the primary and secondary isotherms.

## 3. RESULTS AND DISCUSSION

### 3.1. Interaction of different probe molecules with HY zeolites

The identification and characterization of the Brønsted acid sites in the hydrogen form of Y type zeolites is of significant fundamental interest. A comparative

study of  $\text{NH}_3$ -TPD and CO-TPD on different Y zeolites was presented and discussed in detail in a previous paper.<sup>65</sup> It was shown that carbon monoxide interact with very strong acid sites. In order to better describe the strength distribution of the acid sites, the interaction of *n*-hexane on the same samples as used in the earlier work was investigated in the present study. The temperature programmed desorption experiments were performed after *n*-hexane adsorption on hydrated HY zeolites.<sup>65</sup>

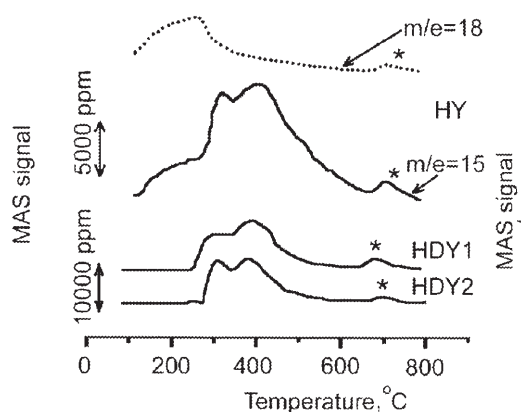


Fig. 1. TPD profiles of ammonia ( $m/e = 15$ ) and water ( $m/e = 18$ ) obtained during temperature programmed heating of  $\text{NH}_4^+$  forms of Y zeolites.

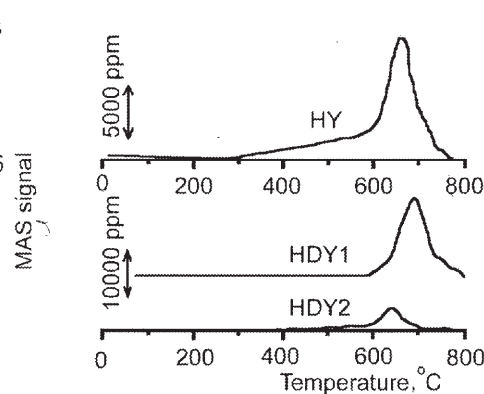


Fig. 2. TPD profiles of CO from HY and HDY samples.

The total number of Brønsted sites was obtained from the mass spectrometric signals of ammonia recorded during temperature programmed heating of  $\text{NH}_4^+$ -exchanged zeolites (Fig. 1). In this way, the TPD spectra of ammonia were monitored in the course of de-ammoniation process. It is well known that  $\text{NH}_4^+$  ions do not exchange with Lewis acid sites. Consequently, the number of acid sites, obtained from the amount of  $\text{NH}_3$  desorbed from  $\text{NH}_4^+$ -exchanged zeolites, presented in Table II, corresponds to the number of Brønsted acid sites. It is worth noticing that, although only slight degrees of de-alumination were achieved, the de-alumination caused the changes in the TPD spectra of ammonia. The desorption starts at higher temperatures and the amounts of desorbed  $\text{NH}_3$  are decreased for the de-aluminated samples. Evidently, two distinguishable regions of  $\text{NH}_3$  desorption exist. The temperature desorption processes of ammonia below 600 °C and the high-temperature desorption process of ammonia around 700 °C. The TPD profiles below 600 °C are very complex, with overlapping peaks and the assignment of particular active centers from the TPD results is very difficult.<sup>8-11</sup> The position of the high-temperature desorption peak of  $\text{NH}_3$  (around 700 °C) is the same as the position of the dehydroxylation peak ( $m/e = 18$ ). The dehydroxylation<sup>10,11</sup> and deammoniation occur from the strongest acid sites. The population of these strongest Brønsted sites,

determined after deconvolution of the TPD spectra, is a small fraction of the total number of sites. The number of NH<sub>3</sub> molecules desorbed per unit cell in the high temperature process is between 1.4 and 2.7, as shown in Table II.

A new insight concerning the Brønsted acid sites on HY and HDY was obtained by TPD of carbon monoxide.<sup>65</sup> It was shown that CO can be successfully used as a probe for studies of the strongest Brønsted sites in zeolites. It was demonstrated that CO is a more sensitive probe for the discrimination of different Brønsted sites than ammonia. A significant amount of CO is adsorbed at 25 °C on HY and HDY zeolites but only a small fraction is chemisorbed (Table I). Profiles of the CO desorption spectra obtained in TPD experiments with HY and HDY samples are presented in Fig. 2. Only high temperature TPD spectra of CO ( $T_m$  in the region 620 – 690 °C) were observed, meaning that CO molecules interact with the very strong acid sites. As can be seen from Fig. 2, the temperature of maximum are only slightly changed after de-alumination. The calculated activation energies for CO desorption which are very high, are presented in Table II. The calculated activation energies confirm that the CO interacted with active sites of similar strength in all the investigated samples ( $E \approx 240$  kJ/mol). Thus, it can be concluded that the interaction of CO molecule with active sites in zeolites is very specific. The unusual strong adsorption of CO seems to be an important finding for the recognition of the strongest Brønsted acid sites.

TABLE II. Quantitative (number of molecules per unit cell) and energetic data (activation energy for desorption) for the adsorption/desorption of ammonia and carbon monoxide

Sample	Si/Al	$N_1$	$N_2$	$N_3$	$N_4$	$E_{act}$ (CO),kJ/mol
HY	2.4	46	2.7	15.6	5.3	242
HDY1	2.6	37	2.6	2.4	0.5	266
HDY2	2.7	35	1.4	2.0	0.2	237

$N_1$  – number of NH<sub>3</sub> molecules desorbed per unit cell during TPD, whole temperature range;  $N_2$  – number of NH<sub>3</sub> molecules desorbed per unit cell, high-temperature process;  $N_3$  – number of CO molecules adsorbed per unit cell at 25 °C;  $N_4$  – number of CO molecules desorbed per unit cell, during TPD.

A recent contribution by W. Markowski<sup>61</sup> reported the application of *n*-hexane-TPD as a method for probing the micropores in zeolites. In that work the TPD of *n*-hexane from ZSM-5 and Y zeolites, previously activated at 400 °C, was studied by the thermogravimetric (TG) method. The typical TPD profiles had a few overlapping peaks. The same effect was also reported by Millot *et al.*<sup>62</sup> The interaction of an alkane with a zeolite is determined by two factors. The first is van der Waals interaction and the second is dipole-induced hydrogen bonding with the Brønsted acid sites.<sup>67</sup> The enthalpy of *n*-hexane adsorption is about 86 kJ/mol and 50 kJ/mol in HZSM-5 and HY zeolites respectively.<sup>68</sup> Consequently, specific interaction of *n*-hexane in zeolites previously covered with water molecules can be expected.

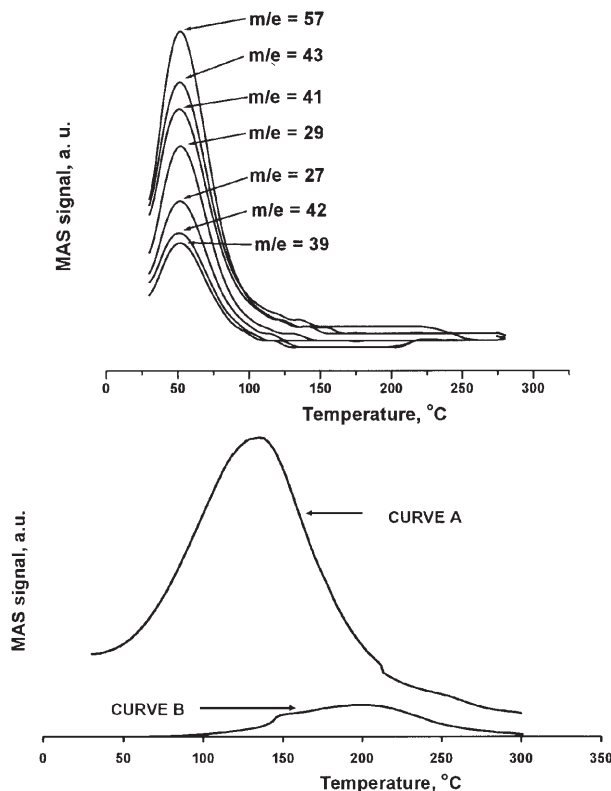


Fig. 3. TPD profiles of a) *n*-hexane ( $m/e = 57, 43, 41, 29, 27, 42$  and  $39$ ) obtained after *n*-hexane adsorption on hydrated HY zeolite; b) water ( $m/e = 18$ ), desorption from HY sample. Curve A: TPD of water obtained for the sample without adsorbed *n*-hexane. Curve B: TPD of water obtained for the sample with adsorbed *n*-hexane.

In order to check the effect of acidity on the adsorption of *n*-hexane on hydrated zeolites, the TPD profiles for water ( $m/e = 18$ ) and hexane were compared (Fig. 3). During the desorption of *n*-hexane from the investigated HY sample, mass originating from the ionization and fragmentation of *n*-hexane molecules in the chamber of the spectrometer ( $m/e = 57$   $C_4H_9$ ,  $m/e = 43$   $C_3H_7$ ,  $m/e = 41$   $C_3H_5$ ) were found. All the monitored signals had the same position and shape. For all *n*-hexane fractions, the desorption profiles were identical, which is an indication of molecular desorption of *n*-hexane. These results indicate that cracking of *n*-hexane, the catalytic reaction often found on acidic zeolites, did not occur during the adsorption of *n*-hexane adsorption on hydrated HY zeolite at room temperature. Only one TPD peak with a maximum at 60 °C was obtained, which is an indication that *n*-hexane is selectively adsorbed at one type of Brønsted acid site.

Typical TPD spectra of water recorded simultaneously with *n*-hexane desorption (curve B) and before *n*-hexane adsorption (curve A) are presented in Fig. 3b, from which it is evident that *n*-hexane adsorption on a hydrated zeolite sample changes the zeolite-water interaction. The TPD profile of water obtained after *n*-hexane adsorption is one symmetric peak shifted towards higher temperatures. It can be concluded that adsorption of *n*-hexane takes place selectively at one type of

the Brønsted acid site, and that there is a competition between *n*-hexane and water molecules for adsorption on these sites. Evidently, *n*-hexane molecules replace previously adsorbed water molecules.

It is clear that the investigated sample had a larger number of sites active for H<sub>2</sub>O adsorption, in comparison to the number of sites active for *n*-hexane adsorption. The results presented hitherto are a clear indication that some Brønsted acid sites are more active for *n*-hexane adsorption than for H<sub>2</sub>O adsorption. Therefore, it could be concluded that *n*-hexane would be adsorbed preferentially in the case of a possible competitive co-adsorption of these two gases.

### 3.2. Interaction of different probe molecules with CuY zeolites

Transition metal modified microporous materials exhibit unique selectivity in catalysis, adsorption science and ion-exchange procedures, as well as significant catalytic activity towards the decomposition of air pollutants (NO<sub>x</sub>, CO<sub>x</sub> and SO<sub>x</sub>).<sup>69</sup> The transition metal particles play the role of active sites in these systems, and their characteristics are usually investigated using nitric oxide and carbon monoxide as probe molecules.

The CO molecule has the ability to act as a weak  $\sigma$ -donor and as a  $\pi$ -acceptor. Thus CO is sensitive to the strong electrostatic fields surrounding transition metal cations in zeolite structures, interacting specifically with cationic Lewis acid sites.<sup>70,71</sup> In previous papers,<sup>44, 72–74</sup> the results of TPD, FTIR and MC investigations of CO interactions with transition metal cation-exchanged FAU and MOR type zeolites were presented and discussed in detail. It was demonstrated that CO interacted at 25 °C with charge-balancing cations, which act as a source of Lewis acidity. High-temperature TPD peaks of CO have been found and interpreted as an indication of the existence of very strong Lewis acidity. The obtained differential heats of adsorption as a function of coverage indicate the heterogeneity of the sites.

In order to check the selectivity of the active sites, in addition to CO, other probe molecules, such as NH<sub>3</sub> and *n*-hexane, were adsorbed on CuY in this study. The TPD profiles for NH<sub>3</sub>, CO and *n*-hexane are compared in Fig. 4. Obviously, all the Lewis acid sites are active for ammonia adsorption. The total amount of ammonia adsorbed on CuY at 100 °C is 46 molecules of NH<sub>3</sub> unit cell. Di-amino complexes are formed between two ammonia molecules bonded to the Cu ion in the CuY zeolite. The TPD MS ( $m/e = 15$ ) profile of ammonia (Fig. 4a) having this broad overlapping peaks in the temperature range from 100 °C to 450 °C clearly indicates the existence of a heterogeneous distribution of the strength of the active sites in the CuY sample, *i.e.*, the interaction of ammonia with the acid sites on CuY zeolite is not selective. The assignment of particular active centers from the TPD of ammonia is very difficult. In order to characterize the specific Lewis sites it is necessary to use some weakly interacting probe molecules. The TPD spectra obtained after CO adsorption on CuY zeolite. The amounts of CO adsorbed (4.5 mole-



cule/unit cell) and desorbed during TPD (4.1 molecule/unit cell) are very similar. Only the signal for  $m/e = 28$  (CO) appeared in the TPD spectrum obtained in the case of CuY. A complex TPD profile, composed of four well-defined peaks ( $T_m = 82, 137, 186$  and  $223$  °C), is obtained. The desorption was completed at  $300$  °C and all peaks had a similar intensity. Hence, the molecularly bound CO was desorbed from four types of active sites, indicating that different types of mono-carbonyl complexes between CO and Cu are formed. This result is in accordance with results obtained from FTIR measurements.<sup>44</sup>

TPD spectra recorded after *n*-hexane adsorption on hydrated CuY zeolite at room temperature are presented in Fig. 4c. The thermodesorption of *n*-hexane monitored in the case of the CuY sample occurs in the same temperature region as the thermodesorption observed in the case of HY zeolites. TPD signals charac-

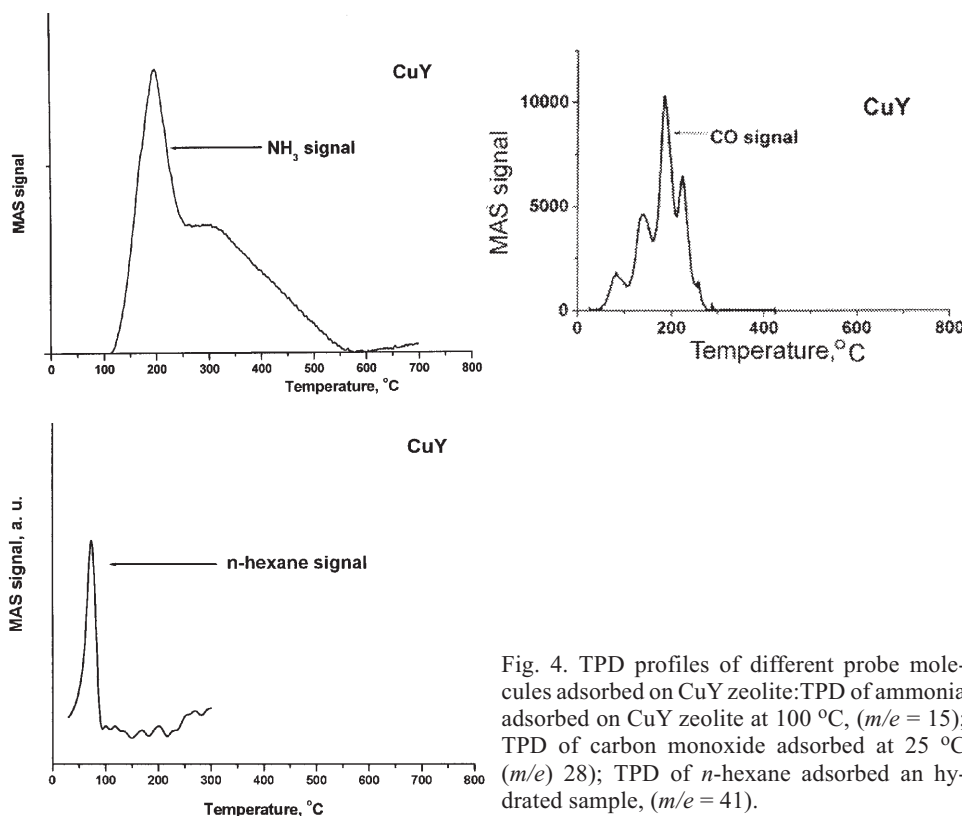


Fig. 4. TPD profiles of different probe molecules adsorbed on CuY zeolite: TPD of ammonia adsorbed on CuY zeolite at  $100$  °C, ( $m/e = 15$ ); TPD of carbon monoxide adsorbed at  $25$  °C ( $m/e = 28$ ); TPD of *n*-hexane adsorbed on a hydrated sample, ( $m/e = 41$ ).

teristic for molecular *n*-hexane ( $m/e = 57, 43, 41, 29, 27, 56, 42, 39$ ) were detected, all with the peak at the same temperature. The TPD peaks are very sharp, indicating a specific interaction *n*-hexane with only one type of sites. In the TPD spectra, signals characteristic for *n*-hexane and fragments which do not belong to the *n*-hexane molecule ( $m/e = 44$ ) were found. The appearance of these signals in TPD spectra is

an indication of *n*-hexane reaction on hydrated CuY zeolite. The investigation of this phenomenon will be published separately. The TPD profiles of water obtained before and after *n*-hexane adsorption, not shown here, are different. *n*-Hexane is selectively adsorbed at one type of Lewis acid site, whereby it replaces previously adsorbed water molecules.

These results indicate that the weakly interacting probe molecules CO and *n*-hexane are much more specific than the strongly interacting NH<sub>3</sub> and, therefore, provide more detailed information about the Lewis acid sites. The TPD studies of *n*-hexane adsorption on a hydrated zeolite surface appear to provide new information about the reactivity of the active sites in CuY zeolite.

### 3.3. Interaction of different probe molecules with HZSM-5-zeolites

For many acid-catalyzed reactions, the catalytic activity increases in order ZSM-5 > MOR > Y type of zeolites. The catalytic activity for *n*-hexane cracking in ZSM-5 zeolite increases linearly with increasing amount of structural aluminum.

The influence of the Si/Al ratio in HZSM-5 zeolites on the number and the strength of acid sites is a subject of our present work. Some averaged features of the active sites in ZSM-5 zeolites can be obtained from calorimetric and TPD studies of ammonia adsorption. TPD studies of *n*-hexane adsorption on a hydrated HZSM-5 zeolite surface appear to provide new information about these sites. The adsorption of ammonia was performed at 150 °C, because the amount of irreversibly adsorbed ammonia at this temperature correlates with the number of strong active sites present.<sup>26</sup>

The dependence of the heat of adsorption on the coverage provides detailed information on the interaction of NH<sub>3</sub> molecules with the active sites in a zeolite. The differential heats of ammonia adsorption on HZSM-5 zeolites with different Si/Al ratio as a function of coverage are shown in Fig. 5. Evidently, the amount of adsorbed ammonia is lower in the case of the more siliceous zeolites. The amounts of irreversibly adsorbed NH<sub>3</sub> are presented in Table III. These results are in accordance with those previously reported in the literature.<sup>76–78</sup> The measured heats of adsorption are indicative of surface homogeneity or heterogeneity in terms of energy distribution, which has been discussed in detail elsewhere.<sup>28,77,78</sup>

A typical differential heat plot shows three regions in the case of a zeolite. The sharp decrease of  $Q_{\text{diff}}$  at low coverage indicates the presence of a small concentration of very strong Lewis type acid sites. The plateau of constant heats of adsorption results from the adsorption of NH<sub>3</sub> on Brønsted-type acid sites. The differential heat then decreases sharply after all the Brønsted-type acid sites were covered.<sup>79</sup> It is noticeable that increasing the Si/Al ratio produced weaker active sites for ammonia adsorption, *i.e.*, the differential heat profiles obtained for HZSM-(120) and HZSM-(28) clearly show a significant increase of  $Q_{\text{diff}}$  in the case of the latter zeolite (Fig. 5). However, it should be noticed here that there is also a decrease of

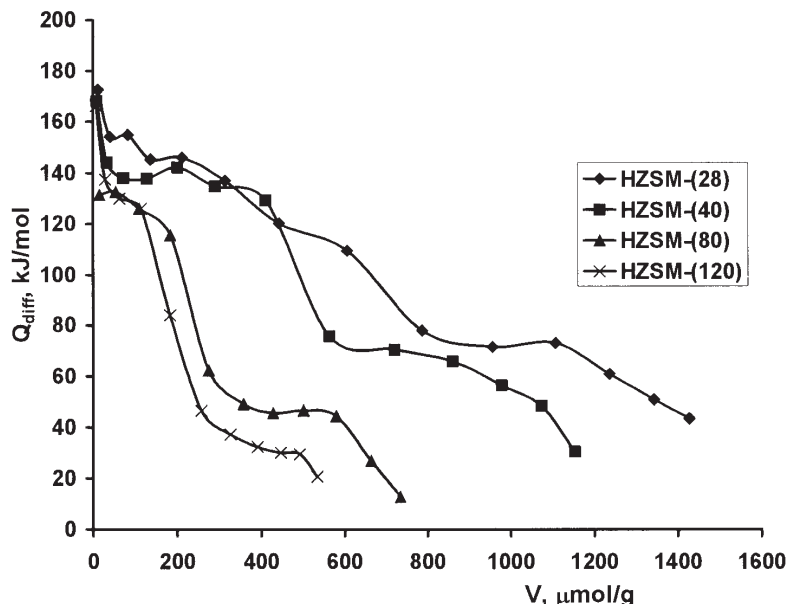


Fig. 5. Differential heats of  $\text{NH}_3$  adsorption at  $150^\circ\text{C}$  as a function of coverage for all HZSM samples.

both the value of  $V_{\text{irr}}$  and the initial differential heat of  $\text{NH}_3$  adsorption in the case of HZSM-(80) and HZSM-(120) (Fig. 5 and Table II). The amount of strongly adsorbed  $\text{NH}_3$  decreased in the following order: HZSM-(28), HZSM-(40), HZSM-(40), HZSM-(80), HZSM-(120).

The  $\text{N}_3$ -TPD profiles of HZSM-5 zeolites with different Si/Al ratio are shown in Fig. 6a. It can be observed that the TPD profiles of ammonia desorbed from the different HZSM zeolites are very similar. All samples exhibit two well resolved desorption peaks: a low-temperature peak (LTP) at *ca.*  $200 - 230^\circ\text{C}$  and a high-temperature peak (HTP) at *ca.*  $400 - 430^\circ\text{C}$ , which is in good agreement with previously published data.<sup>80</sup> Generally, the LTP and HTP correspond to weak and strong acid sites, respectively. Similar  $\text{NH}_3$ -TPD curves have been previously reported for HZSM-5 zeolites, where higher adsorption temperatures (*i.e.*,  $150 - 200^\circ\text{C}$ ) and longer stripping times, *i.e.*, (1 – 2 h) under high vacuum were used.<sup>81,82</sup>

The *n*-hexane TPD spectra ( $m/e = 41$ ) of all the investigated HZSM samples are shown in Fig. 6b. These results clearly indicate that the number and strength of the acid sites accessible for hexane differ for hydrated HZSM zeolites with different Si/Al ratio. The profiles are complex and consist of at least two or three overlapping peaks, which is a clear indication of the energetic heterogeneity of the sites accessible for *n*-hexane. Two well resolved peaks centered at about  $120^\circ\text{C}$  and at  $200^\circ\text{C}$  are observed in the spectra of the HZSM-(80) and HZSM-(120) zeolites. The peaks appearing at about  $120^\circ\text{C}$  and at lower temperatures corresponding to

sites of low/medium acid strength, while the peaks at 200 °C can be attributed to strong acid sites. The TPD profiles of *n*-hexane desorption from hydrated HZSM zeolites are generally similar to the results obtained for dehydrated silicalite (activated at 400 °C), published by B. Millot *et al.*<sup>61</sup>

TABLE III. Quantitative ( $\mu\text{mol/g}$ , number of molecules per unit cell) data on  $\text{NH}_3$ ,  $\text{N}_2\text{O}$  and CO adsorption on HZSM and CuZSM zeolites

Sample	Si/Al	$V_1$	$N_1$	$V_2$	$N_2$	$V_3$	$N_3$
HZSM-(28)	28	1150					
HZSM-(40)	40	800					
HZSM-(80)	80	600					
HZSM(120)	120	400					
CuZSM-(79)	50	542	2.1	41.3	0.16	130	0.50
CuZSM-(128)	50	542	1.5	41.8	0.10	269	0.66
CuZSM-(150)	50	545	1.1	7.3	0.015	243	0.50

$V_1 - V_{\text{irr}}$  ( $\mu\text{mol NH}_3/\text{g}$ );  $V_2 - V_{\text{irr}}$  ( $\mu\text{mol N}_2\text{O}/\text{g}$ );  $V_3 - V_{\text{irr}}$  ( $\mu\text{mol CO}/\text{g}$ );  $N_1$  -  $\text{NH}_3$  molecules/Cu ion;  $N_2$  -  $\text{N}_2\text{O}$  molecules/Cu ion;  $N_3$  - CO molecules/Cu ion

Simultaneously with *n*-hexane desorption, the TPD spectra for water ( $m/e = 18$ ) were recorded (results not shown here). It should be pointed out that differences in the TPD spectra of water desorbed from sample which had and had not been exposed to *n*-hexane were observed. These results will be discussed separately.

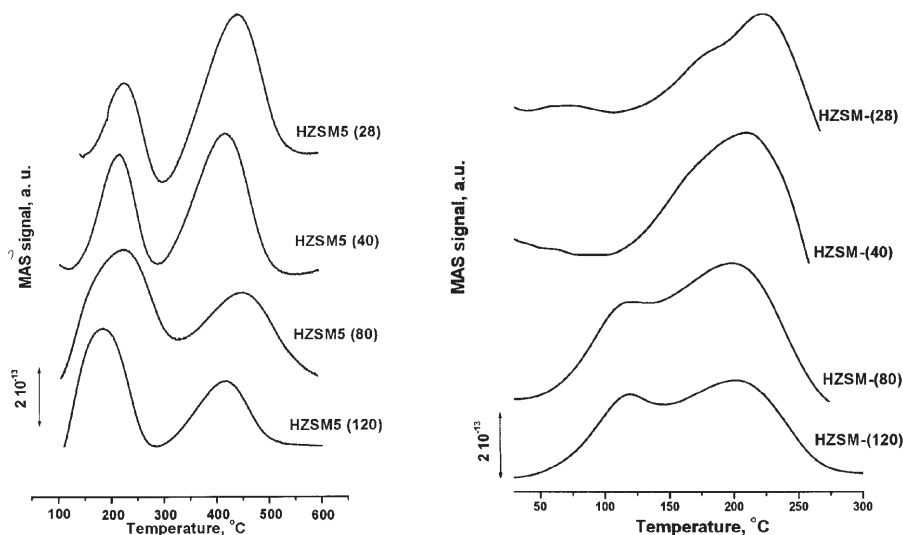


Fig. 6. TPD profiles of a)  $\text{NH}_3$ ; b) *n*-hexane from HZSM samples.

### 3.4. Interaction of different probe molecules with CuZSM-5 zeolites

High-silica zeolites modified by transition metal cations possess unusual catalytic properties which are quite different from those of low-silica zeolites modified with the same cations. It is generally accepted that CuZSM-5 zeolite is the most efficient catalysts for  $\text{NO}_x$  decomposition.<sup>83–85</sup> The adsorption behavior of Cu(II) ion-exchanged ZSM-5 samples with different copper loadings was investigated previously.<sup>66</sup> The adsorptions of  $\text{N}_2\text{O}$  and CO at 25 °C were studied using the calorimetric method and infrared spectroscopy. Copper ion-exchanged ZSM-5 zeolites were prepared with different copper loadings, from under- to over-exchanged levels.<sup>66, 86</sup> A comparison of the amounts of  $\text{NH}_3$ ,  $\text{N}_2\text{O}$  and CO adsorbed on the same sample was also made. The adsorbed amounts decreased in the following sequence:  $\text{NH}_3$ , CO,  $\text{N}_2\text{O}$ .

The results obtained from FTIR experiments clearly show that the active sites for both  $\text{N}_2\text{O}$  and CO are Cu(I) ions, which were formed by reduction in a dynamic vacuum during the activation procedure (at 400 °C).<sup>66</sup> It was also evidenced that the Cu(I) active sites have different strengths of interaction with the adsorbed molecules, most probably due to their different localization in the zeolite framework.

The amounts of irreversibly desorbed gases were different (see Fig. 7 and Table III). The amount of ammonia adsorbed at the strong sites in all the investigated samples was  $\approx 550 \mu\text{mol/g}$ . Di-amino complexes were formed between two ammonia molecules strongly bonded to the Cu ion in the CuZSM-(79) sample, while in the case of CuZSM-(150), only one ammonia molecule was chemisorbed per Cu ion. The influence of the level of ion-exchange is evidenced in the CO adsorption experiments. The increase of the irreversibly adsorbed amount of CO,  $V_{\text{irr}}$  in the case of CuZSM-(128) compared with that for CuZSM-(79) is proportional to the increase of the copper content, while there was no significant increase of  $V_{\text{irr}}$  in the case of CO adsorption on CuZSM-(150) sample. The amount of irreversibly adsorbed strongly bonded CO was less than 1 CO molecule per Cu ion. However, these numbers were higher than in the case of  $\text{N}_2\text{O}$  adsorption, indicating a higher affinity of the active sites for CO adsorption. The amount of  $\text{N}_2\text{O}$  adsorbed was 41  $\mu\text{mol/g}$  for both the under and slightly over-exchanged CuZSM samples. It is evident from the results presented in Table III that only a small number of the strong active sites, were available for adsorption of  $\text{N}_2\text{O}$  on the investigated samples. Evidently, nitrous oxide molecules cannot access all the copper ions in the structure of the over-exchanged sample CuZSM-(150).

The profiles of differential heat *versus* gas uptake ( $\mu\text{mol/g}$ ) obtained in this work for  $\text{NH}_3$ ,  $\text{N}_2\text{O}$  and CO adsorption on all CuZSM-(*x*) samples are presented in Fig. 7. The profiles of the differential heats of the employed probe molecules are not similar. The possibility to insight the heterogeneity of the active sites depends on the employed probe molecule. The obtained results indicate again the existence of different distributions of the strength of the acid sites, and the influence of Cu ion content. The heterogeneity could be explained by different coordination, acce-

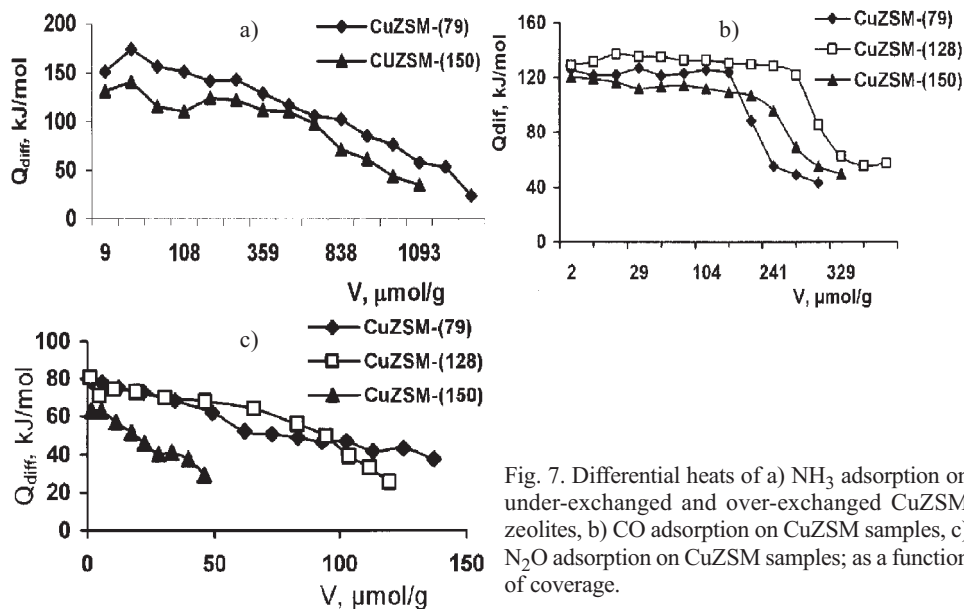


Fig. 7. Differential heats of a)  $\text{NH}_3$  adsorption on under-exchanged and over-exchanged CuZSM zeolites, b) CO adsorption on CuZSM samples, c)  $\text{N}_2\text{O}$  adsorption on CuZSM samples; as a function of coverage.

ssibility and binding properties of the Cu ions, arising from their different positions in the ZSM-5 framework.

The initial values of  $Q_{diff}$  obtained in the case of CO adsorption are similar to those obtained for  $\text{NH}_3$ . The interaction of CO and the Lewis sites formed in the Cu exchanged ZSM-5 zeolite is very strong.<sup>87</sup> According to the consideration published by Zecchina<sup>31</sup> carbon monoxide seems to be the best choice to probe Lewis acid sites.

The values of the differential heat of  $\text{N}_2\text{O}$  adsorption in the investigated systems show that these interactions are weaker than those with CO and  $\text{NH}_3$ .

Differential heats of  $\text{N}_2\text{O}$  adsorption between 80 and 30 kJ/mol were determined. Taking into account the amounts of irreversibly adsorbed  $\text{N}_2\text{O}$  it can be inferred that only those  $\text{N}_2\text{O}$  molecules bonded with a differential heat higher than 60 kJ/mol were chemisorbed.

The hitherto presented results are a clear indication that  $\text{Cu}^+$  ions, produced by reduction of  $\text{Cu}^{2+}$  ions in ion-exchanged zeolite samples, are stronger active sites in CO adsorption than in  $\text{N}_2\text{O}$  adsorption. An important observation is that the application of different probe molecules, on the one hand ammonia, which is able to access all the acid sites, and on the other hand, CO, which can attach to the very strong Lewis sites, and  $\text{N}_2\text{O}$ , which can only be adsorbed on very specific sites, enables a deep insight to be obtained about the existence of active sites in the case of the investigated systems.

*n*-Hexane -TPD profiles of hydrated Cu-exchanged ZSM-5 zeolites are shown in Fig. 8. In the spectrum of CuZSM-(79) (which is similar to that of CuZSM-(128), it can be observed that a well-resolved symmetric peak dominates with a maximum at about 175 °C, while shoulder appears at 85 °C. Two types of (weak and medium) acid

sites accessible for *n*-hexane adsorption can be distinguished. In these experimental TPD curves. In the case of sample CuZSM-(150), with a high concentration of Cu ions only one broad peak at 160 °C exists. As the content of Cu in the ZSM-5 samples increases, the main peak becomes smaller and less well-resolved while its maximum also shifts to slightly lower temperature region as was observed for the HZSM-5 series.

The hiterto presented results are a clear indication that *n*-hexane can attach to the Brønsted or Lewis acid sites even when the zeolite channels are occupied with water molecules. The hydrated CuZSM-5 and HZSM-5 zeolite are more strongly active for *n*-hexane adsorption than hydrated CuY and HY type zeolites. In the *n*-hexane TPD spectra on Y type zeolite, only one peak at 60 – 70 °C exist. The

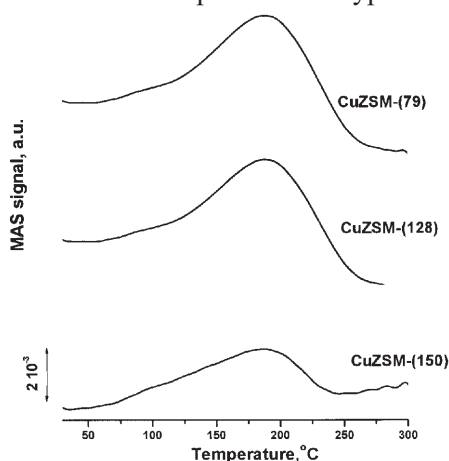


Fig. 8. TPD profiles of *n*-hexane ( $m/e = 41$ ) obtained for CuZSM samples (the profiles of other characteristic fragments of *n*-hexane are omitted for clarity since they are the same as  $m/e = 41$ ).

present results are consistent with the enthalpy of *n*-hexane adsorption in HZSM-5 and HY zeolites, 86 kJ/mol and 50 kJ/mol respectively.<sup>68</sup> The van der Waals and dipole-induced hydrogen bonding interactions of *n*-hexane molecule with the acid sites are dependent on the zeolite framework.

#### 4. CONCLUSION

Several techniques aimed at probing the environments surrounding the Brønsted and Lewis sites have been described. It was shown that the heterogeneity of the sites depends on the employed probe molecule and also changes with the content of Cu and H ions in the zeolite structure. Some averaged feature of the adsorption capabilities can be obtained from calorimetric studies and from TPD studies using ammonia. The adsorption of CO and N<sub>2</sub>O at room temperature provides information about the nature and accessibility of the sites. Moreover, TPD studies of *n*-hexane adsorption on hydrated zeolite surfaces appear to provide an exciting new method for obtaining information about the active sites. The adsorption complexes in the system water–hexane–zeolite should be finally characterized by <sup>1</sup>H, <sup>13</sup>C-NMR measurements.

In the present study, molecular *n*-hexane was successfully used as a probe for the investigation of Y and ZSM-5 zeolites. It was found that in Y and ZSM-5 zeolites, some of the sites adsorb molecular *n*-hexane, even though the zeolites were covered with water.

The unusually strong adsorption of *n*-hexane on hydrated zeolite samples seems to be an important discovery for designing new catalytic processes.

## ИЗВОД

УПОРЕДНО ИСПИТИВАЊЕ АКТИВНИХ ЦЕНТАРА ЗЕОЛИТА  
РАЗЛИЧИТИМ ПРОБНИМ МОЛЕКУЛИМА

ВЕРА ДОНДУР,<sup>1</sup> ВЕСНА РАКИЋ,<sup>2</sup> ЉИЉАНА ДАМЈАНОВИЋ,<sup>1</sup> и АЛИНЕ АУРОУХ<sup>3</sup>

<sup>1</sup>Факултет за физичку хемију, Свуденски брз 12-16, 11000 Београд, <sup>2</sup>Пољопривредни факултет, Немањина 6, 11080 Београд-Земун, Србија и Црна Гора и <sup>3</sup>Institut de Recherches sur la Catalyse, 2 Av. A. Einstein, 69626 Villeurbanne, France

У овом раду је приказан преглед испитивања киселих активних центара код зеолита ZSM-5 и Y температурски програмираном десорпцијом (TPD) и адсорпционом микрокалориметријом уз коришћење различитих пробних молекула: NH<sub>3</sub>, CO, N<sub>2</sub>O и *n*-хексана. Први пут је показана адсорпција *n*-хексана на киселим центрима хидратисаних зеолита.

(Примљено 14. децембра 2004)

## REFERENCES

1. A. Corma, *Chem. Rev.* **95** (1995) 559
2. P. T. Anastas, L. B. Barlet, M. M. Kirschoff, T. C. Williamson, *Catal. Today* **55** (2000) 11
3. W. E. Farneth, R. J. Gorte, *Chem. Rev.* **95** (1995) 615
4. N. Y. Topsoe, F. Joensen, E. G. Derouane, *J. Catal.* **110** (1988) 404
5. N. Nesterenko, F. Thiabult-Strarzyk, V. Montouillout, V. Yuschenko, C. Fernandez, J. Gilson, F. Fajula, I. Ivanova, *Micropor. Mesopor. Mater.* **71** (2004) 157
6. M. Huang, S. Kaliaguine, A. Auroux, *J. Phys. Chem.* **99** (1995) 9952
7. E. G. Derouane, *Chem. Phys. Lett.* **142** (1987) 200
8. H. Karge, V. Dondur, J. Weitkamp, *J. Phys. Chem.* **95** (1991) 283
9. H. Karge, V. Dondur, *J. Phys. Chem.* **94** (1990) 765
10. M. Neuber, V. Dondur, H. Karge, L. Pacheco, S. Ernst, J. Weitkamp, *Stud. Sur. Sci. and Catal.* **37** (1988) 461
11. V. Dondur, H. Karge, *Surf. Sci.* **190** (1987) 873
12. C. Costa, I. Dzhikh, J. Lopes, F. Lemos, F. Ribeiro, *F. R. J. Mol. Catal. A. Chem.* **154** (2000) 193
13. J. Hoffmann, B. Hunger, U. Streller, Th. Stock, D. Dombrowski, A. Barth, *Zeolites* **5** (1985) 31
14. B. Hunger, J. Hoffmann, O. Heitzsc, M. Hunger, *J. Therm. Anal.* **36** (1990) 1379
15. K. Koch, B. Hunger, O. Klepel, M. Heuchel, *J. Catal.* **172** (1997) 187
16. B. Hunger, M. Heuchel, L. Clark, R. Snur, *J. Phys. Chem. B* **106** (2002) 3882
17. F. Lonyi, J. Vallyon, *Micropor. Mesopor. Mater.* **47** (2001) 293
18. V. Solinas, I. Ferino, *Catal. Today* **41** (1998) 179
19. B. E. Spiewak, J. A. Dumesic, *Thermochim. Acta* **290** (1996) 435
20. J. A. Lercher, C. Grunding, G. Eder-Mirth, *Catal. Today* **27** (1996) 353
21. A. Auroux, *Stud. in Sur. Sci. and Cat.*, P. J. Grobet, W. J. Morier, E. F. Vansant and G. Schulz-Elkoff, Eds., Elsevier, **37** (1988), p. 385



22. W. Farneth, R. Gorte, *Chem. Rev.* **95** (1995) 615
23. Y. Kuroda, Y. Yoshikawa, R. Kumashiro, M. Nagao, *J. Phys. Chem. B* **101** (1997) 6497
24. A. Bore'ave, A. Auroux, C. Giuman, *Micropor. Mesopor. Mater.* **11** (1997) 275
25. B. Spiewak, B. Handy, S. Sharma, J. Dumesic, *Catal. Lett.* **23** (1994) 207
26. A. Auroux, *Top. Catal.* **4** (1997) 71
27. A. Auroux, Y. Ben Taarit, *Thermochim. Acta* **122** (1987) 63
28. A. Auroux, *Top. Catal.* **19** (2002) 205
29. A. Zecchina, C. Otero Arean, *Chem. Soc. Rev.* (1996) 187
30. E. Brunner, *Catal. Today* **38** (1997) 361
31. A. Zecchina, C. Lamberti, S. Bordiga, *Catal. Today* **41** (1998) 169
32. G. Catana, D. Baetens, T. Mommaerts, R. Shoonheydt, B. Weckhuysen, *J. Phys. Chem. B* **105** (2001) 4904
33. H. Knozinger, S. Huber, *J. Chem. Soc. Faraday Trans.* **94** (1998) 2047
34. B. S. Shete, V. S. Kamble, N. M. Gupta, V. B. Kartha, *J. Phys. Chem. B* **102** (1998) 5581
35. Y. Kuroda, Y. Yoshikawa, R. Kumashiro, M. Nagao, *J. Phys. Chem. B* **101** (1997) 6497
36. A. Zecchina, S. Bordiga, G. Spoto, L. Marchese, G. Pterini, G. Leofant, M. Padovan, *J. Phys. Chem.* **96** (1992) 4991
37. M. A. Makarova, K. M. Al-Gefaili, J. Dwyer, *J. Chem. Soc. Faraday Trans.* **90** (1994) 383
38. Y. Kuroda, T. Mori, Y. Yoshikawa, S. Kittaba, R. Kumashiro, M. Nagao, *Phys. Chem. Phys.* **1** (1999) 3807
39. E. Garrone, B. Fubini, B. Bonelli, B. Onida, C. O. Area'n, *Phys. Chem. Chem. Phys.* **1** (1999) 573
40. R. Gorote, D. White, *Micropor. Mesopor. Mater.* **35** (2000) 447
41. W. Zhang, X. Han, X. Liu, *J. Mol. Catalysis A: Chemical* **194** (2003) 107
42. W. Zhang, X. Han, X. Liu, X. Bao, *Micropor. Mesopor. Mater.* **50** (2001) 13
43. E. Brunner, *J. Mol. Struct.* **355** (1995) 61
44. V. Rakić, R. Hercigonja, V. Dondur, *Micropor. Mesopor. Mater.* **27** (1999) 27
45. K. Krisna, G. B. F. Seijger, C. M. van den Bleek, M. Makkee, Guido Mul, *H. P. A. Calis, Cat. Lett.* **86** (2003) 121
46. H. Knozinger, in *Handbook of Heterogeneous Catalysis*, Vol. 2, G. Ert, H. Knozinger, J. Weitkamp, Eds., VCH, Weinheim, 1997, p. 707
47. P. T. Fanson, M. W. Stradt, J. Lanterback, W. Nickolas Delgass, *Appl. Catal. B: Environ.* **38** (2002) 331
48. M. Shimokanwabe, K. Hirano, N. Takezawa, *Catal. Today.* **45** (1998) 117
49. N. U. Zhanpeisov, W. S. Ju, M. Matsouka, M. Anpo, *Struct. Chem.* **14** (2003) 247
50. X. Solans-Monfort, M. Sodupe, V. Branchadell, *Chem. Phys. Lett.* **368** (2003) 242
51. B. L. Su, V. Norberg, *Langmuir* **14** (1998) 2352
52. G. Turnes-Palomino, P. Fisticaro, S. Bordiga, A. Zecchina, E. Giamello, C. Lamberti, *J. Phys. Chem. B* **104** (2000) 4064
53. Z. Sobalik, J. Dedecek, I. Ithonnikov, B. Wichterlova, *Micropor. Mesopor. Mater.* **21** (1998) 525
54. B. Wichterlova, J. Dedecek, Z. Sobalik, A. Vondrova, K. Klier, *J. Catal.* **169** (1997) 194
55. J. Dedecek, Z. Sobalik, Z. Tvarnzikova, D. Kancky, B. Wichterlova, *J. Phys. Chem.* **99** (1995) 16327
56. Y. Kuroda, Y. Yoshikawa, R. Kumashiro, M. Nagao, *J. Phys. Chem. B* **101** (1997) 6497
57. A. Gervasini, C. Picciau, A. Auroux, *Micropor. Mesopor. Mater.* **35/36** (2000) 457
58. D. Olson, P. Reischman, *Zeolites* **17** (1996) 434
59. F. Eder, J. A. Lercher, *Zeolites* **18** (1997) 75
60. F. Eder, M. Stockenhuber, J. A. Lercher, *J. Phys. Chem. B* **101** (1997) 5414
61. B. Millot, A. Methivier, H. Jobic, *J. Phys. Chem. B* **103** (1998) 3210
62. W. Makowski, D. Majda, *Thermochim. Acta* **412** (2004) 131
63. S. Savitz, A. L. Myers, R. J. Gorte, *Micropor. Mesopor. Mater.* **37** (2000) 33
64. A. Serykh, V. Kazansky, *Phys. Chem. Chem. Phys.* **6** (2004) 5250
65. V. Rakić, V. Dondur, R. Hercigonja, V. Andrić, *J. Thermal Analysis and Calorimetry* **72** (2003) 761

66. V. Rakić, V. Dondur, S. Gajinov, A. Auroux, *Thermochim. Acta* **420** (2004) 51
67. J. A. van Bokhoven, B. A. Williams, W. Ji, D. Koningsberger, H. Kung, J. Miller, *J. Catal.* **224** (2004) 50
68. S. M. Babitz, B. A. Williams, J. T. Miller, R. Q. Snurr, W. O. Hagg, H. H. Kung, *Appl. Catal. A* **179** (1999) 71
69. M. Iwamoto, *Stud. Surf. Sci. Catal.* **84** (1994) 1395
70. K. I. Hadžiivanov, M. M. Kantcheva, D. G. J. Klissurski, *J. Chem. Soc. Faraday Trans.* **92** (1996) 4595
71. A. Corma, *Chem. Rev.* **95** (1995) 559
72. V. Rakić, V. Dondur, R. Hercigonja, *Thermochim. Acta* **77** (2001) 349
73. V. Rakić, V. Dondur, U. Mioč, D. Jovanović, *Top. Catal.* **19** (2002) 241
74. V. Rakić, V. Dondur, R. Hercigonja, *J. Serb. Chem. Soc.* **68** (2003) 409
75. J. A. van Bokhoven, B. A. Williams, W. Ji, D. C. Koningsberger, H. H. Kung, J. T. Miller, *J. Catal.* **224** (2004) 50
76. A. Jentis, J. A. Lercher, *Stud. Surf. Sci. Catal.* **137** (2001) 345
77. P. Carniti, A. Gervasini, A. Auroux, *J. Catal.* **150** (1994) 274
78. P. Carniti, A. Gervasini, A. Auroux, *Langmuir* **17** (2001) 6938
79. B. Dragoi, A. Gervasini, E. Dumitriu, A. Auroux, *Thermochim. Acta* **420** (2004) 127
80. K. Wendlandt, H. Toufar, B. Unger, W. Schwieger, K. Berg, *J. Chem. Soc. Faraday Trans.* **87** (1991) 2507
81. H. G. Karge, L. C. Jozefowicz, *Stud. Surf. Sci. Catal.* **84** (1994) 685
82. S. Sharma, B. Meyers, D. Chen, J. Miller, J. Dumesic, *Appl. Catal. A: General* **102** (1993) 253
83. J. Zhang, M. Flytzani-Stephanopoulos, *J. Catal.* **164** (1996) 131
84. Z. Schay, L. Guzzi, A. Beck, J. Nagy, V. Samuel, S. P. Mirajkar, A. V. Ramasvamy, G. Pal-Barbely, *Catal. Today* **75** (2002) 393
85. M. Iwamoto, H. Yakiro, K. Tanda, N. Mizono, Y. Mine, S. Kagawa, *J. Phys. Chem.* **95** (1991) 3727
86. V. Rakić, V. Dondur, S. Gajinov, A. Auroux, *Materials Science Forum* **453** (2004) 83
87. V. Bolis, A. Barbaglia, S. Bordiga, C. Lamberti, A. Zecchina, *J. Phys. Chem. B* **108** (2004) 9970.